DOI: 10.1002/ejic.201100953

Synthesis of Rhenium(I) Tricarbonyl Complexes with Carbohydrate-Pendant Tridentate Ligands and Their Cellular Uptake

Yuji Mikata,*[a] Kyoko Takahashi,[b] Yuka Noguchi,[b] Masami Naemura,[b] Anna Ugai,[b] Saori Itami,[c] Keiko Yasuda,[c] Satoshi Tamotsu,[c] Takashi Matsuo,[d] and Tim Storr[e]

Keywords: Sugar–metal hybrid material / Carbohydrates / Glycosides / Rhenium / Ligand effects

Twelve $[Re^{I}\mathbf{L}(CO)_3]^{n+}$ complexes with various carbohydrate-pendant ligands **L** have been prepared and their uptake into HeLa S3 cells were investigated. The ligand library includes: (i) glucose/galactose as the carbohydrate group; (ii) bis(2-pyridylmethyl)amine (DPA), bis(2-quinolylmethyl)amine (DQA), or *N*-(2-pyridylmethyl)glycine (NPG) as the metal binding component; and (iii) an ethylene chain as a linker between the metal binding site and the *O*/*C*-glycosides. Microwave induced plasma mass spectroscopy (MIP-MS) measurements revealed that all complexes were extensively incorporated into the HeLa cells over a 24 h period, and the DQA complexes showed the highest uptake of all the complexes in the series. However, in comparison to the corresponding Re complexes without the pendant carbohydrate functions (prepared with the related ligands $\mathbf{L}^{DPA}$, $\mathbf{L}^{DQA}$, and $\mathbf{L}^{NPG}$), only the NPG complexes exhibited carbohydrate enhanced cellular uptake. Considering their water solubility and cellular uptake properties, the NPG complexes containing an *O*-glycoside group (**L1** and **L′1**) are the best candidates for enhancing cellular uptake of metal ions. Microscopic analysis with PC-12 cells in the presence of the fluorescent complex $[Re(\mathbf{L'7})(CO)_3]Cl$, revealed that the complex stays in the cell cytosol and cannot penetrate into the nucleus.

Introduction

Functionalized carbohydrates are of significant interest as building blocks for high order complex carbohydrate structures, asymmetric catalysts, and sugar-metal hybrid materials.[1] The attachment of carbohydrate moieties to functional molecules provides integrated properties such as water solubility, chirality, and biological recognition elements to those materials. The most convenient and inexpensive strategy to access carbohydrate functionalized materials is a pendant approach in which functional molecules are connected via a linker to commercially available carbohydrates.[2]

The radiopharmaceutical application of group VII metals such as ^{99m}Tc and $^{186/188}$Re is of recent interest. ^{99m}Tc has ideal properties ($t_{1/2}$ = 6.01 h, γ = 142.7 keV) for use in single photon emission computed tomography (SPECT). Convenient isolation from a ^{99}Mo generator justifies the extensive use of ^{99m}Tc in medical imaging methods. ^{186}Re ($t_{1/2}$ = 3.68 d, β = 1.07 MeV, γ = 137 keV) and ^{188}Re ($t_{1/2}$ = 16.98 h, β = 2.12 MeV, γ = 155 keV) have potential use in therapeutic nuclear medicine. The $[M(CO)_3]^+$ (M = Tc, Re) core has received considerable attention due to its small size, inert d^6 low-spin configuration, and simple aqueous chemistry.[3] Tridentate chelates are well suited for binding to the $[M(CO)_3]^+$ core, providing a high level of stability to the resultant complexes due to the chelate effect and by limiting the accessibility of the metal center to endogenous ligands in vivo. The rational design of ligands for radioisotopes with diagnostic/therapeutic properties is highly desirable, especially for use in imaging and therapy. Extensive studies have been accumulated, and several carbohydrate functionalized complexes have been reported that display benefits, in addition to those mentioned above, due to their carbohydrate groups.[2d,4]

In this article, facile synthetic routes to tridentate carbohydrate-pendant ligands (Scheme 1) are reported. The ligand library includes: (i) glucose/galactose as a carbohydrate moiety; (ii) DPA, DQA, or NPG as the metal binding component; and (iii) an ethylene linker between the metal binding site and the *O*/*C*-glycosides. Attachment of carbohydrate functions to the ligands, especially glucose analogs, was hypothesized to enhance the water solubility and more importantly membrane permeability via cellular glucose transporters (GLUT) of the compounds,[5] although some carbohydrate-pendant complexes have been reported

[a] KYOUSEI Science Center, Nara Women's University, Nara 630-8506, Japan
Fax: +81-742-203-095
E-mail: mikata@cc.nara-wu.ac.jp
[b] Department of Chemistry, Nara Women's University, Nara 630-8506, Japan
[c] Department of Biological Sciences, Nara Women's University, Nara 630-8506, Japan
[d] Graduate School of Materials Science, Nara Institute of Science and Technology (NAIST), Takayama, Ikoma, Nara 630-0192, Japan
[e] Department of Chemistry, Simon Fraser University, 8888 University Drive, Burnaby, BC, V5A-1S6, Canada
Supporting information for this article is available on the WWW under http://dx.doi.org/10.1002/ejic.201100953.

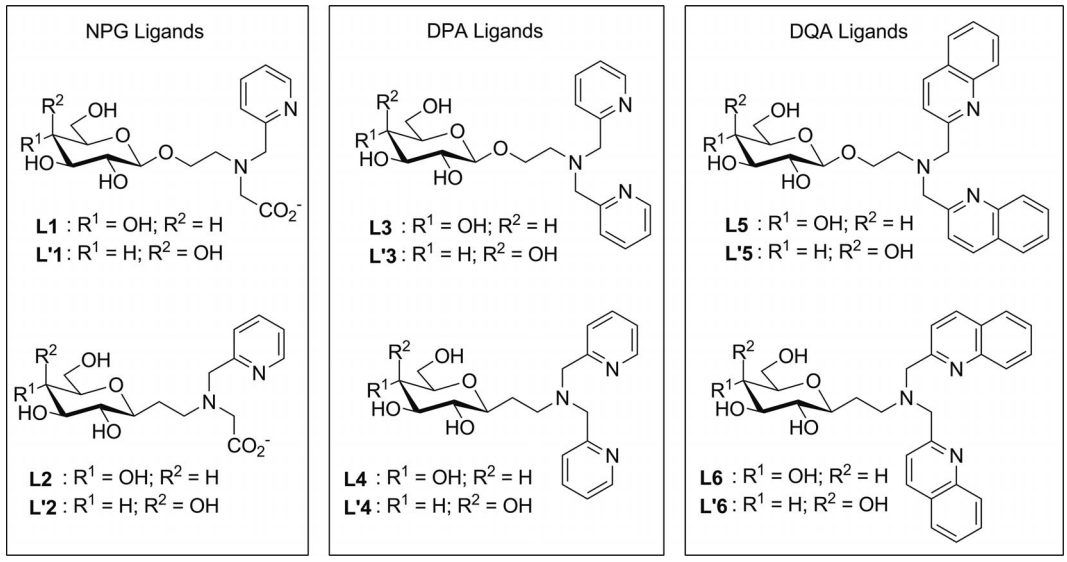

Scheme 1.

to have neither recognition nor transportation ability via the Glut1 transporter.[6] *C*-Glycosides are the carbon analogs of naturally occurring *O*-glycosides and have been extensively studied because of their chemical and enzymatic stability.[7] This paper provides efficient strategies for carbohydrate functionalization of rhenium(I) tricarbonyl complexes, and details of the cellular uptake analyses, performed with HeLa cells, of these complexes.

Results and Discussion

Synthesis of the Ligands

Carbohydrate-pendant ligands **L1**–**6** and **L′1**–**6** were synthesized according to Schemes 2–4. The preparations of **L3** and **L′3** have been reported previously.[8] Ligands **L1H** and **L′1H** were synthesized from 2-bromoethyl 2,3,4,6-tetra-*O*-acetyl-β-D-gluco- or galactopyranoside (**1/1′**)[8] that were reacted with *N*-(2-pyridylmethyl)glycine *tert*-butyl ester,[9] a procedure that was then followed by deprotection of the carboxylate and sugar hydroxy groups (Scheme 2). The other ligands, **L2H**, **L′2H L4**–**6** and **L′4**–**6**, were prepared by alkylation of carbohydrate-tethered primary amines **7**/**7′** (Scheme 3) and **11/11′**[10] (Scheme 4) with 2 equiv. of an alkylating agent – 2-(chloromethyl)pyridine, 2-(chloromethyl)quinoline, or *tert*-butyl bromoacetate – followed by deprotection. The preparation of *C*-glucosylamine **7** has been reported previously.[11] The *C*-galactosylamine **7′** was obtained by a procedure similar to the one given in that report. During the preparation of **7/7′**, the cyanomethyl *C*-glycosides **6/6′**[11–12] formed as crystals suitable for X-ray crystallography, and Figures S1 and S2 reveal the molecular structures of **6** and **6′**, including the β-configuration of the carbohydrate groups. It should be mentioned that compounds **8/8′** were obtained from a one-pot reaction involving amines **7/7′** that were reacted with 1 equiv. of 2-chloromethylpyridine and 1 equiv. of *tert*-butyl bromoacetate; **8/8′**

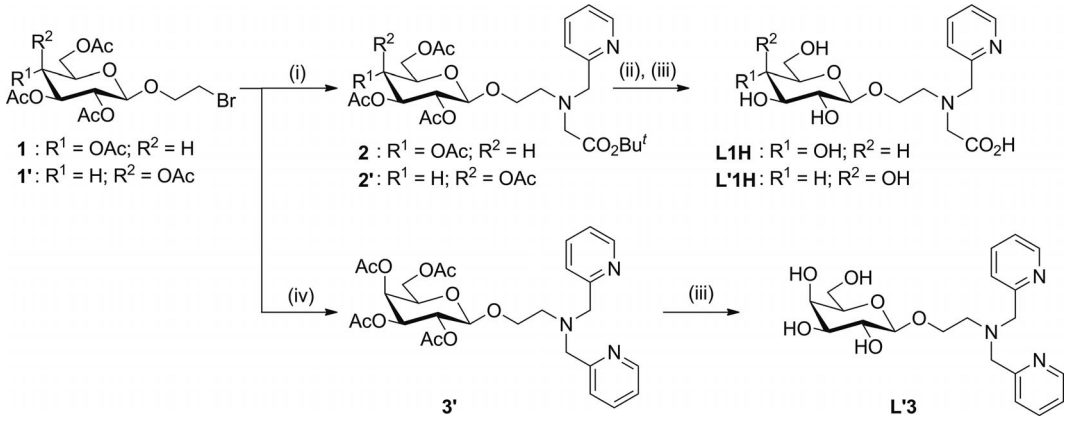

Scheme 2. *Reagents and conditions:* (i) *N*-(2-pyridylmethyl)glycine *tert*-butyl ester, DMF; (ii) formic acid; (iii) NaOMe, MeOH; (iv) bis(2-pyridylmethyl)amine.

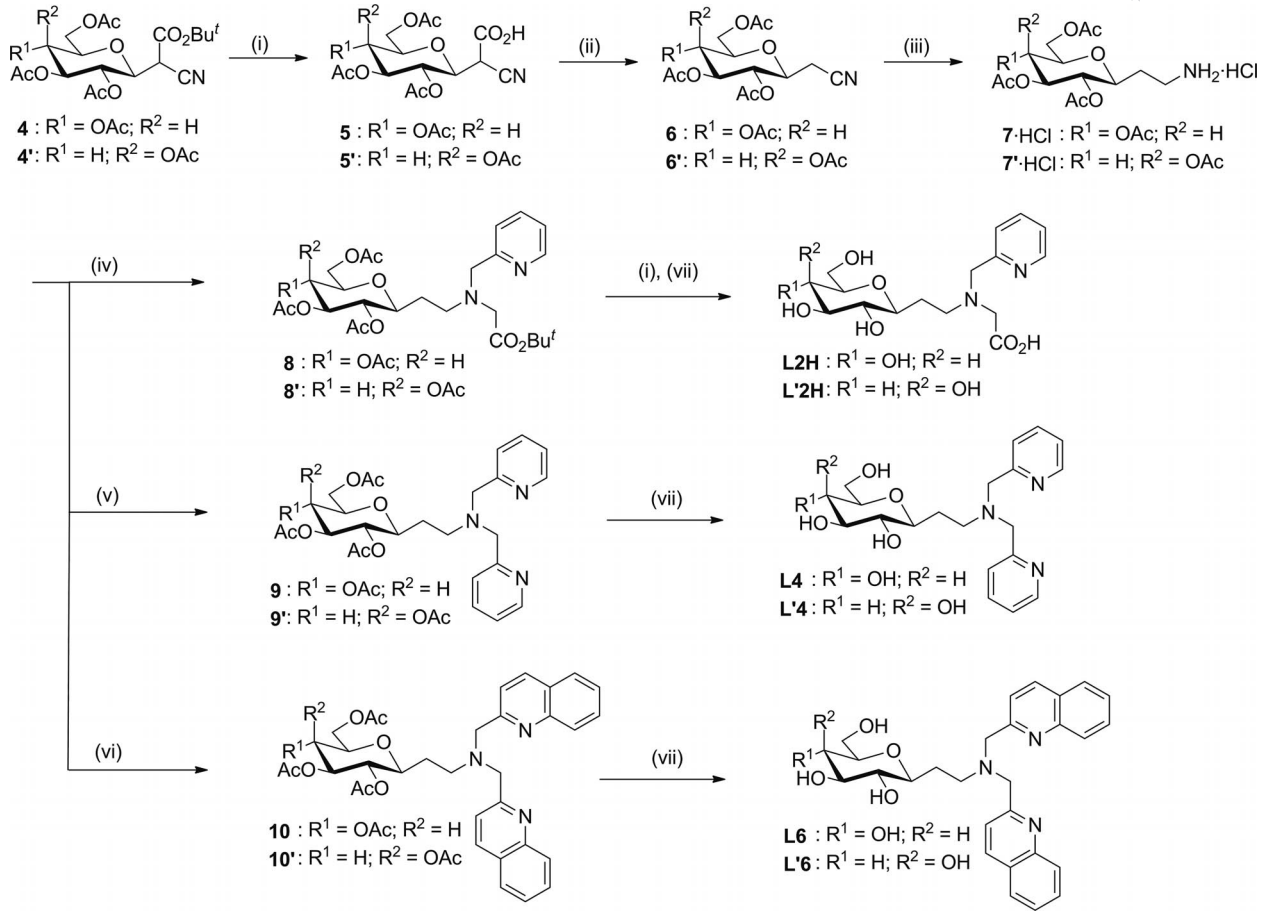

Scheme 3. *Reagents and conditions:* (i) formic acid; (ii) diisopropylethylamine (DIPEA); (iii) H_2, PtO_2, $CHCl_3$/EtOH; (iv) 2-(chloromethyl)-pyridine, *tert*-butyl bromoacetate, dimethylformamide (DMF); (v) 2-(chloromethyl)pyridine, DMF; (vi) 2-(chloromethyl)quinoline, DMF; (vii) NaOMe, MeOH.

were obtained in good yields (69–88%) and no significant amount of side products were isolated. The results of ^{1}H/^{13}C NMR, ESI-MS, and elemental analyses supported the proposed structures for all ligands.

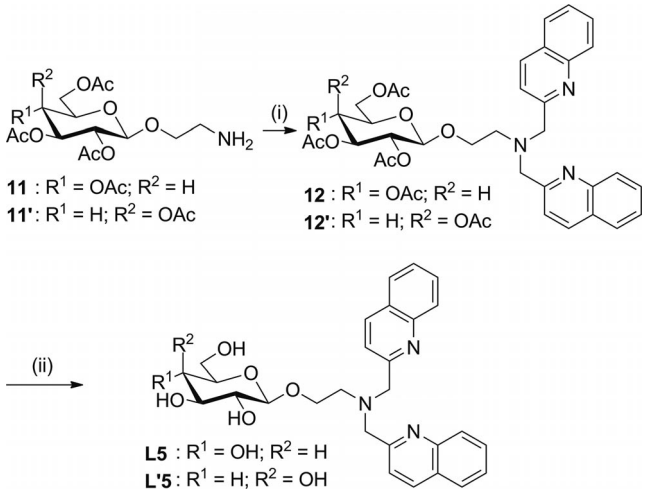

Scheme 4. *Reagents and conditions:* (i) 2-(chloromethyl)quinoline, DMF; (ii) NaOMe, MeOH.

The ethylamine derivatives shown in Scheme 5 that contain the same metal binding sites as **L1**–**6**/**L′1**–**6** but no sugar residues were prepared. $\mathbf{L^{DPA}}$ is a known compound,[13] but the other two ligands ($\mathbf{L^{NPG}H}$ and $\mathbf{L^{DQA}}$) were synthesized for the first time and fully characterized, details of which are provided in this paper. The crystal structure of $\mathbf{L^{DQA}}$ was also determined (see Supporting Information, Table S1 and Figure S3).

Synthesis of the Rhenium(I) Tricarbonyl Complexes

Ligands **L1**–**6** and **L′1**–**6** were refluxed with rhenium pentacarbonyl chloride to afford [Re**L**$(CO)_3$] for **L1**,**2**/**L′1**,**2** or [Re**L**$(CO)_3$]Cl for **L3**–**6**/**L′3**–**6** in 31% to quantitative yield. As represented in the ^{1}H NMR spectrum of [Re(**L4**)$(CO)_3$]Cl shown in Figure 1, distinct chemical shift changes for the protons associated with the metal binding are observed when the ligand binds to the metal. No significant chemical shift changes were observed for the carbohydrate protons. This clearly shows that the rhenium centers in the present complexes coordinate to the tridentate metal binding sites via the nitrogen or oxygen atoms, and confirms that the carbohydrate moieties remain pendant. In

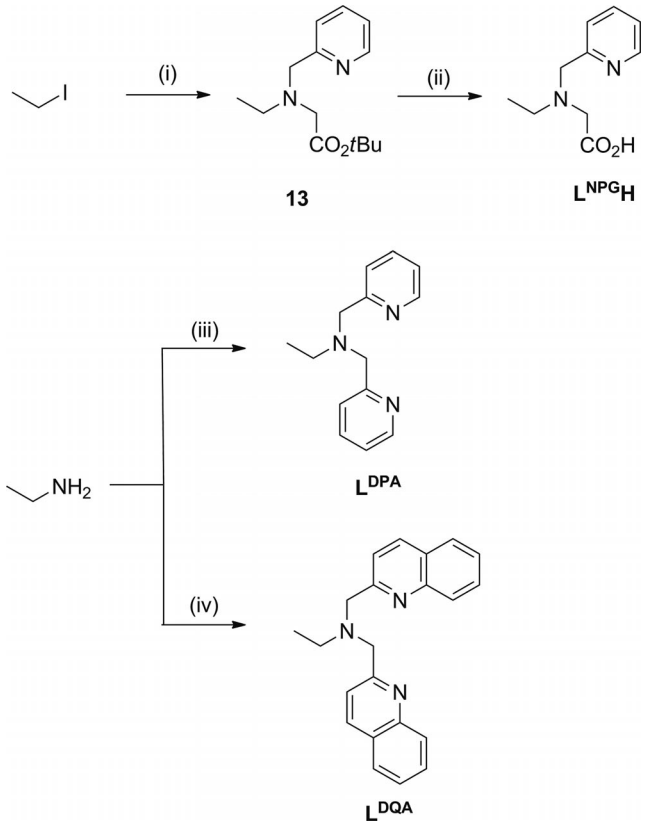

Scheme 5. *Reagents and conditions:* (i) *N*-(2-pyridylmethyl)glycine *tert*-butyl ester, DMF; (ii) trifluroacetic acid (TFA); (iii) 2-(chloromethyl)pyridine, acetonitrile; (iv) 2-(chloromethyl)quinoline, acetonitrile.

Figure 1, the py3 signal, which exhibits a clear doublet in the spectrum of the free ligand, displays further splitting in the spectrum of the complex, this is likely to be due to the long-range effect of the carbohydrate chirality within the more rigid metal chelate. In the NPG complexes, the metal coordinated nitrogen atoms become chiral centers. In this study we did not see any further splitting of the NMR signals, suggesting the exclusive formation of one diastereomer for each of the NPG complexes. But we could not determine the absolute configuration of the complexes. The results from $^{1}H/^{13}C$ NMR, ESI-MS, and elemental analyses supported the proposed structures for all complexes.

Crystal structure elucidation was successfully performed for the *C*-glycoside complex [Re(**L′4**)(CO)$_3$]Cl, and confirmed the above mentioned structure (Figure 2). The Re complex of compound **9** {[Re(**9**)(CO)$_3$]ClO$_4$} with a OH-protected *C*-glucoside group also afforded crystals suitable for X-ray crystallography (Figure 3). These structures exhibit no significant changes from the corresponding *O*-glycoside derivatives, indicating the stable coordination of the tridentate *N*,*O*-ligands that support the rhenium tricarbonyl structure.

The analogous rhenium complexes without the pendant sugar moieties were prepared in a similar way to that employed for the preparation of the **L1**–**6** and **L′1**–**6** complexes detailed above. All complexes were fully characterized by $^{1}H/^{13}C$ NMR, ESI-MS, and elemental analyses, and [Re(**L**^{NPG})(CO)$_3$]Cl and [Re(**L**^{DPA})(CO)$_3$]Cl were also analyzed by X-ray crystallography (Figures S4 and S5, Supporting Information).

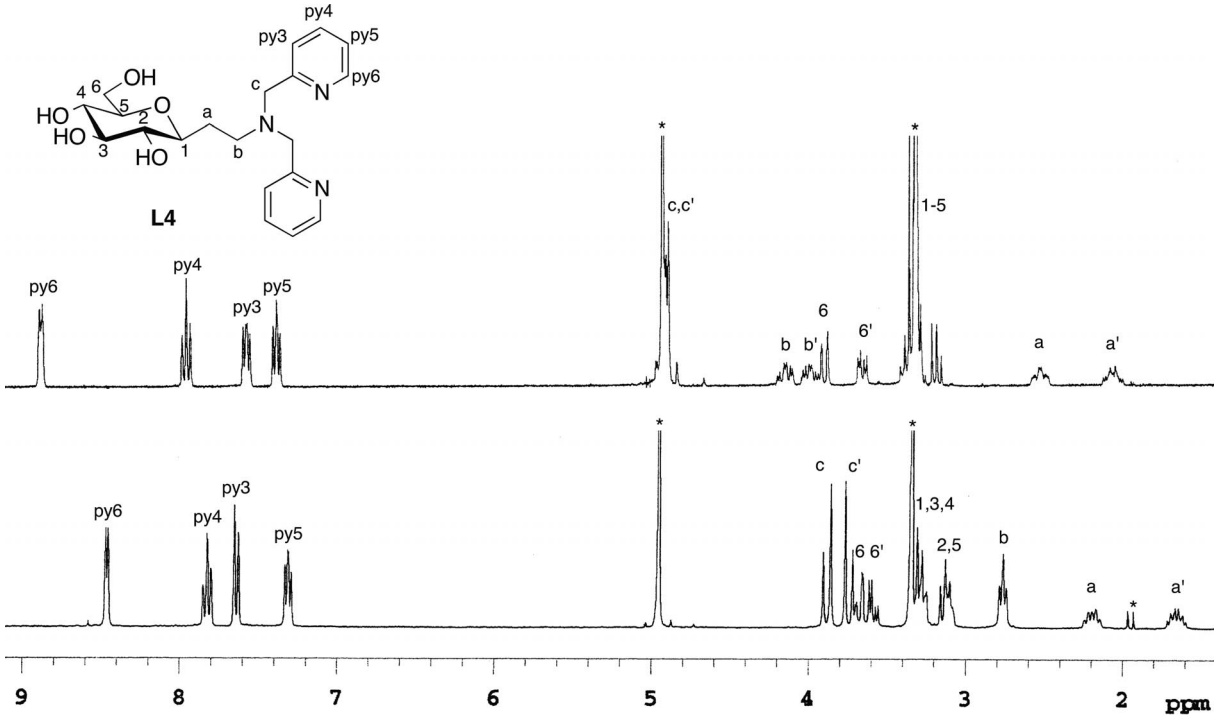

Figure 1. Partial ^{1}H NMR spectra for [Re(**L4**)(CO)$_3$]Cl (top) and **L4** (bottom) in CD$_3$OD. Asterisks indicate solvent peaks or those associated with small amounts of impurities.

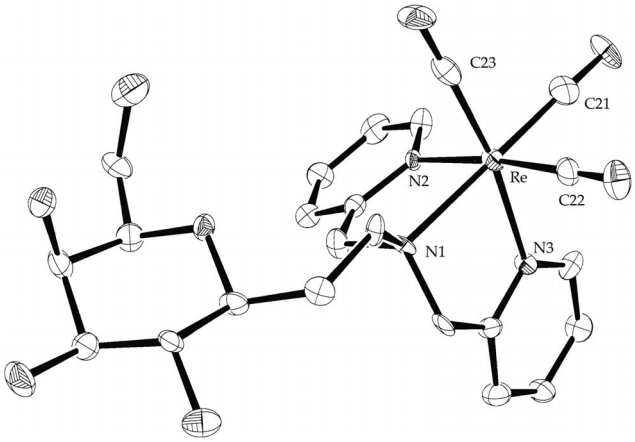

Figure 2. ORTEP diagram of the cationic portion of $[Re(\mathbf{L'4})(CO)_3]$-$Cl{\cdot}0.5CH_3CN{\cdot}0.5C_2H_5OH$ (ellipsoids are drawn at the 50% probability level). The hydrogen atoms, counter anion, and solvent molecules are omitted for clarity.

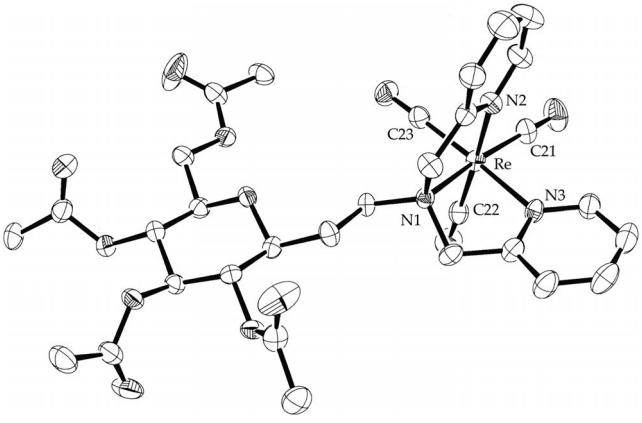

Figure 3. ORTEP diagram of the cationic portion of $[Re(\mathbf{9})(CO)_3]$-$ClO_4{\cdot}H_2O$ (ellipsoids are drawn at the 50% probability level). The hydrogen atoms, counter anion, and solvent molecule are omitted for clarity.

MIP-MS Evaluation of the Uptake of Re Complexes by HeLa S3 Cells

Quantification of rhenium metal uptake into HeLa S3 cells was investigated, allowing for evaluation of the effect of the ligand structure on the uptake process. Fifteen Re complexes with and without pendant carbohydrate moieties were incubated with the cells at 100 μM concentration in growth media for 24 h, and the incorporated metal contents in the cells were quantified by MIP-MS. No detectable cytotoxicity of the complexes was observed under the experimental conditions used. The results of this study are shown in Table 1 and summarized in Figure 4. The cell volume (2.27 pL) was calculated from the mean radius (16.3 μm) of the cells measured by microscopic analysis, and with the assumption that the cells are spherical in shape.

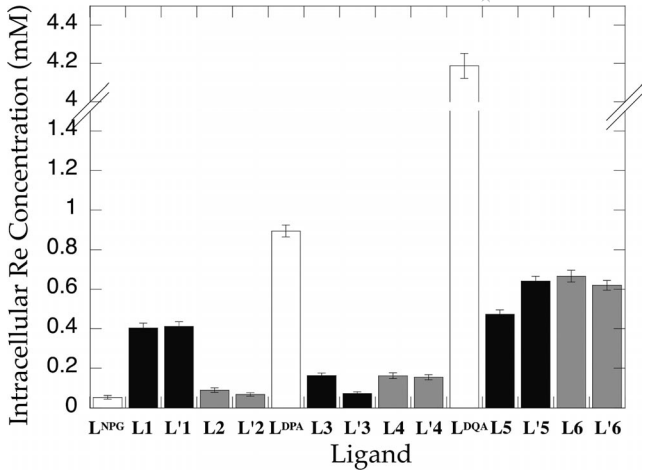

Figure 4. Cellular rhenium concentration (mM) after incubation for 24 h of HeLa S3 cells with the Re^I tricarbonyl complexes (100 μM) containing sugar-pendant ligands. Open bars, filled bars, and gray bars represent nonsugar, *O*-glycoside, and *C*-glycoside ligands, respectively.

The rhenium complexes without pendant carbohydrate functions exhibit considerable differences in the amount of cellular uptake when compared to their carbohydrate-appended analogues. The Re complexes of $\mathbf{L^{DPA}}$ and $\mathbf{L^{DQA}}$ exhibit higher uptake values (Figure 4) in comparison to the carbohydrate-attached complexes, probably because of their increased hydrophobicity. It is of significant interest that in the NPG derivatives, for which all complexes have good water solubility, the pendant *O*-glycoside in **L1/L′1** enhances Re incorporation into the cells by a factor of 5–8 compared with the *C*-glycoside and nonsugar analogues. This *O*-glycoside preference was not observed in the DPA and DQA series. Finally, in all cases no significant difference between the glucose and galactose derivatives was observed.

Considering the total charge of the complex, the cell membrane permeability trend would be expected to be as follows: NPG complexes (neutral chelate) > DPA and DQA complexes (cationic metal chelates). However, the present results show that the overall trend in Re complex uptake is DQA > DPA > NPG and there is little difference in the uptake of the the *C*- and *O*-glycosides. Because the DQA complexes exhibit poor water solubility, the high water solubility of the NPG complexes is of significant importance. Interestingly, the NPG *O*-glycoside derivatives (**L1/L′1**) exhibit enhanced uptake in comparison to both the *C*-glycoside analogues (**L2/L′2**) and the carbohydrate-free derivative. The effect of *O*-glycosylation of the ligands in the NPG series causes a deviation from the overall trend observed for metal complex uptake, and provides a potential starting point for further structural modifications aimed at enhancing the cellular uptake of rhenium(I) tricarbonyl complexes. Increased glucose concentration in media did not block the uptake of the **L1** and **L′1** complexes (data not shown), suggesting that the uptake mechanism is different from that for glucose transport.

Table 1. Details of the uptake of Re^{I} tricarbonyl complexes by HeLa S3 Cells.[a]

Ligand	Re [ng L^{-1}], individual	Re [ng L^{-1}], average	Re uptake (nmol/10^5 cells)	Cellular concentration of Re (mM)[b]
$\mathbf{L^{NPG}}$	234.5 ± 37.0 217.0 ± 30.5 233.0 ± 42.0	228.0 ± 36.5	(1.22 ± 0.20) × 10^{-2}	0.054 ± 0.009
L1	1654.0 ± 108.5 1797.5 ± 103.0 1663.0 ± 98.5	1705.0 ± 103.0	(9.16 ± 0.55) × 10^{-2}	0.404 ± 0.024
L′1	1648.0 ± 80.5 1771.0 ± 87.5 1804.0 ± 127.0	1741.0 ± 98.0	(9.35 ± 0.53) × 10^{-2}	0.412 ± 0.023
L2	435.5 ± 50.0 352.0 ± 46.0 338.5 ± 47.5	375.5 ± 48.0	(2.02 ± 0.26) × 10^{-2}	0.089 ± 0.011
L′2	296.0 ± 34.5 298.5 ± 34.5 271.0 ± 33.0	288.5 ± 34.0	(1.55 ± 0.18) × 10^{-2}	0.068 ± 0.008
$\mathbf{L^{DPA}}$	3959.5 ± 131.5 3612.0 ± 117.5 3747.5 ± 122.5	3773.0 ± 124.0	(20.26 ± 0.67) × 10^{-2}	0.893 ± 0.030
L3	702.0 ± 49.5 653.5 ± 53.5 707.5 ± 61.0	687.5 ± 55.0	(3.69 ± 0.30) × 10^{-2}	0.163 ± 0.013
L′3	294.0 ± 36.0 319.0 ± 24.5 303.0 ± 38.5	305.0 ± 33.0	(1.64 ± 0.18) × 10^{-2}	0.072 ± 0.008
L4	616.9 ± 59.0 691.5 ± 61.0 745.5 ± 63.5	684.5 ± 61.0	(3.68 ± 0.33) × 10^{-2}	0.162 ± 0.015
L′4	670.5 ± 65.0 621.0 ± 55.0 673.0 ± 48.5	655.0 ± 56.0	(3.52 ± 0.30) × 10^{-2}	0.155 ± 0.013
$\mathbf{L^{DQA}}$	21303.0 ± 414.0 17067.0 ± 110.0 14723.0 ± 303.5	17698.0 ± 276.0	(95.04 ± 1.48) × 10^{-2}	4.187 ± 0.065
L5	1991.5 ± 87.5 2080.5 ± 93.0 2010.0 ± 115.0	2000.5 ± 98.5	(10.74 ± 0.53) × 10^{-2}	0.473 ± 0.023
L′5	3174.5 ± 108.0 2373.5 ± 105.0 2581.0 ± 100.5	2709.5 ± 104.5	(14.55 ± 0.56) × 10^{-2}	0.641 ± 0.025
L6	2702.0 ± 135.5 2863.5 ± 110.5 2880.0 ± 137.5	2815.0 ± 128.0	(15.12 ± 0.69) × 10^{-2}	0.666 ± 0.030
L′6	2688.5 ± 83.5 2574.5 ± 117.5 2605.0 ± 115.0	2622.5 ± 105.0	(14.08 ± 0.56) × 10^{-2}	0.620 ± 0.025

[a] Recorded after 24 h incubation. [b] The average volume of the cells was estimated to be 2.27 pL (see text).

Evaluation by Fluorescent Microscopy of the Uptake of Re Complexes by PC-12 Cells

The distribution of a representative Re complex inside PC-12 cells was investigated by a fluorescent microscopy measurement[14] performed with a methoxy substituted DQA *O*-galactoside complex, [Re(**L′7**)$(CO)_3$]Cl (Scheme 6), for which superior cell uptake and fluorescence detection was expected. Introduction of the methoxy group on to the quinoline ring enhances the fluorescent intensity and shifts the excitation/emission wavelengths of the ligand relative to the signals for the corresponding ligand devoid of such a group.[15] Considering the "*O*-glycoside effect" observed for the **L1**/**L′1** complexes, the *O*-glycoside linker was chosen for use in this study.

Upon excitation at 330 nm, [Re(**L′7**)$(CO)_3$]Cl exhibited a moderately intense fluorescence signal at around 420 nm (Figure S6), which can be viewed by a fluorescent microscope (excitation 330–385 nm, detection > 420 nm). The fluorescent microscopic analysis was performed with PC-12 rat adrenal pheochromocytoma. Increased fluorescence from the cells was observed after incubation with [Re(**L′7**)$(CO)_3$]Cl (50 μM) for 4 h (Figure 5, b). From this picture we can conclude that the complex penetrates into the cell because the fluorescence was observed from whole cell and not localized in the cell membrane. The fluorescent nuclear stain DAPI (4′,6-diamino-2-phenylindole dihydrochloride) was added during the microscopic analysis and selectively accumulates in the cell nucleus (Figure 5, c). Interestingly, overlaying of parts b and s of Figure 5 demon-

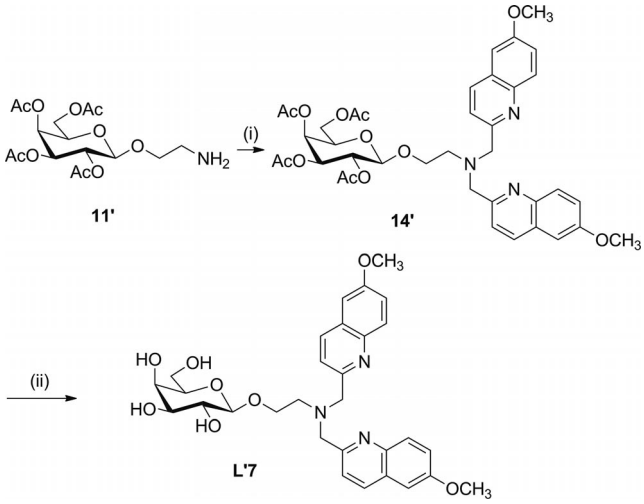

Scheme 6. *Reagents and conditions:* (i) 2-(chloromethyl)-6-methoxyquinoline, DMF; (ii) NaOMe, MeOH.

strates that [Re(**L′7**)(CO)$_3$]Cl is localized in the cytosol and does not penetrate into the nucleus (Figure 5, d). This study clearly demonstrates the cell permeability of [Re(**L′7**)(CO)$_3$]Cl and also the localization of the complex in PC-12 cells.

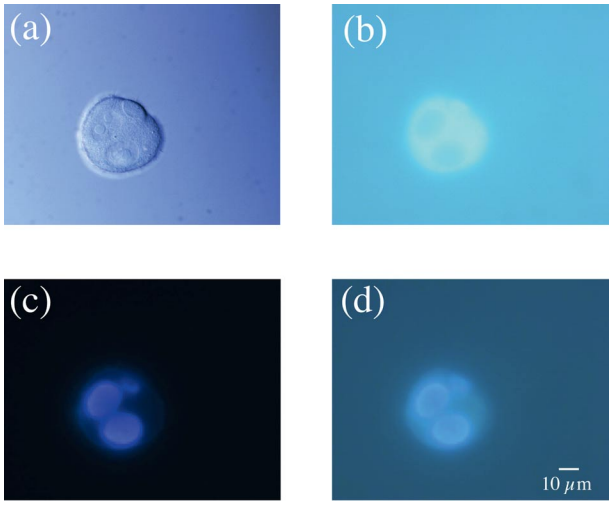

Figure 5. Differential interference contrast and fluorescent micrographs of cultured PC-12 rat adrenal cells incubated in the presence of [Re(**L′7**)(CO)$_3$]Cl (50 μM) for 4 h: (a) differential interference contrast; (b) fluorescent micrograph; (c) fluorescent micrograph in the presence of DAPI; (d) image formed from the merging of images (b) and (c).

Conclusions

Glucose- and galactose-pendant ligands containing DPA, DQA, and NPG as metal binding sites have been prepared. The structures of rhenium(I) tricarbonyl complexes with these ligands were characterized and their uptake into HeLa S3 cells studied. MIP-MS measurements reveal that the DQA complexes show the highest uptake of all the complexes in the series. Microscopic analysis with the fluorescent quinoline derivative [Re(**L′7**)(CO)$_3$]Cl reveals that the complex stays in the cytosol and does not penetrate into the nucleus. The water soluble NPG complexes exhibited carbohydrate enhanced cell uptake; however, no carbohydrate dependent uptake was observed in this study. The NPG complexes with pendant *O*-glycoside groups, **L1** and **L′1**, displayed increased uptake in comparison to both the *C*-glycoside analogues (**L2**/**L′2**) and the carbohydrate-free derivative. This result provides a potential starting point for further structural modifications aimed at enhancing the cellular uptake of rhenium(I) tricarbonyl complexes. We are currently investigating the cellular uptake of the Re complexes in a variety of cell lines to determine the generality of this approach. Biodistribution studies employing radioactive ^{99m}Tc complexes are also currently underway.

Experimental Section

General: All reagents and solvents for the syntheses were obtained from commercial sources and used as received. ^{1}H NMR (300.07 MHz) and ^{13}C NMR (75.00 MHz) spectra were recorded on a Varian GEMINI 2000 spectrometer and referenced to internal tetramethylsilane (TMS) or solvent signals. Elemental analyses were recorded on a J-Science JM-10 Micro Corder. The synthetic and characterization details for all new compounds are described in the Supporting Information.

X-ray Crystallography: Single crystals of **6**, **6′**, **L^{DQA}**, [Re(**L′4**)(CO)$_3$]Cl, [Re(**9**)(CO)$_3$]ClO$_4$, [Re(**L^{NPG}**)(CO)$_3$]Cl, and [Re(**L^{DPA}**)(CO)$_3$]Cl were covered by Paraton-N oil and mounted on glass fibers. All data were collected at 123 or 223 K on a Rigaku Mercury charge coupled device (CCD) detector, with monochromatic Mo-K_α radiation generated from an X-ray tube operating at 50 kV/40 mA. Data were processed on a PC with the CrystalClear Software (Rigaku). Structures were solved by direct methods (SIR-92)

Table 2. Crystallographic data for [Re(**L′4**)(CO)$_3$]Cl·0.5CH$_3$CN·0.5C$_2$H$_5$OH and [Re(**9**)(CO)$_3$]ClO$_4$·H$_2$O.

	[Re(**L′4**)(CO)$_3$]Cl·0.5CH$_3$CN·0.5C$_2$H$_5$OH	[Re(**9**)(CO)$_3$]ClO$_4$·H$_2$O
Formula	$C_{25}H_{31.5}ClN_{3.5}O_{8.5}Re$	$C_{31}H_{37}ClN_3O_{17}Re$
FW	738.70	945.30
Crystal system	monoclinic	monoclinic
Space group	*C*2	$P2_1$
a [Å]	36.4467(14)	14.271(2)
b [Å]	9.2658(4)	7.3184(9)
c [Å]	16.1508(7)	19.286(3)
β [deg]	95.546(2)	111.1690(12)
V [Å^3]	5428.7(12)	1878.4(4)
Z	8	2
$D_{calcd.}$ [g cm^{-3}]	1.807	1.671
μ [cm^{-1}]	46.335	33.838
$2\theta_{max}$ [deg]	55.0	55.0
Temperature [K]	123	223
Reflections collected	21484	14746
Reflections used	11713	8649
R_{int}	0.0322	0.0224
Parameters	712	506
Final *R*1[a] [$I > 2\theta(I)$]	0.0399	0.0307
*wR*2[a] (all data)	0.0806	0.0659
GOF	1.067	1.047

[a] $R1 = (\Sigma||F_o| - |F_c||)/(\Sigma|F_o|)$. $wR2 = \{[\Sigma w(F_o^2 - F_c^2)^2]/[\Sigma w(F_o^2)^2]\}^{1/2}$.

and refined by full-matrix least-squares methods on F^2 (SHELXL-97). Crystal data for carbohydrate-pendant rhenium(I) tricarbonyl complexes [Re(**L′4**)(CO)$_3$]Cl and [Re(**9**)(CO)$_3$]ClO$_4$ are summarized in Table 2. Crystallographic data for **6**, **6′**, $\mathbf{L^{DQA}}$, [Re($\mathbf{L^{NPG}}$)(CO)$_3$]Cl, and [Re($\mathbf{L^{DPA}}$)(CO)$_3$]Cl are provided in Tables S1 and S2 of the Supporting Information, and their ORTEP drawings are given in Figures S1–5.

CCDC-825160 {for [Re(**9**)(CO)$_3$]ClO$_4$}, -825161 {for [Re(**L′4**)(CO)$_3$]Cl}, -825162 {for [Re($\mathbf{L^{NPG}}$)(CO)$_3$]Cl}, -825163 {for [Re($\mathbf{L^{DPA}}$)(CO)$_3$]Cl}, -825164 (for **6**), -825165 (for **6′**), -825166 (for $\mathbf{L^{DQA}}$) contain the supplementary crystallographic data for this paper. These data can be obtained free of charge from The Cambridge Crystallographic Data Centre via www.ccdc.cam.ac.uk/data_request/cif.request/cif.

Cellular Uptake Analyses with HeLa S3 Cells: HeLa S3 cells (100,000 cells/well) were cultured in Minimum Essential Medium (MEM) supplemented with 10% fetal bovine serum (FBS), penicillin (100 U/mL) and streptomycin (0.1 mg/mL). All cells were maintained in a humidified incubator at 37 °C under 5% CO_2. The media was changed to one containing the Re complexes (100 μM) and the cells incubated for 24 h. The well was treated with trypsin for 10 min at 37 °C, and then the cells were collected by centrifuge (1,200 rpm, 5 min) and washed with Phosphate Buffered Saline (PBS) (1 mL, 3 times). The collected cells were added to mili-Q water (50 μL) and concentrated HNO_3 (100 μL). After being heated at 95 °C for 2 h, the solution was diluted to 10 mL with water, and the rhenium content was analyzed with a Hitachi MIP-MS P-6000 Microwave Induced Plasma Mass Spectrometer (NAIST). The average values of three independent experiments with standard deviations are given in Table 1.

Fluorescent Microscopic Analysis with PC-12 Cells: PC-12 rat adrenal pheochromocytoma cells were cultured in Roswell Park Memorial Institute (RPMI) 1640 supplemented with 5% fetal bovine serum (FBS), 10% horse serum (HS) and 1% penicillin-streptomycin (PS). All cells were maintained in a humidified incubator at 37 °C under 5% CO_2. The media was changed to one containing [Re(**L′7**)(CO)$_3$]Cl (50 μM) and the cells incubated for 4 h. The cells were rinsed with FBS, soaked in the growth media, and then analyzed with a fluorescent microscope (excitation filter: OLYMPUS BP330–385, detection filter: BA420). DAPI was added to the cells during the microscopic analysis to enable identification of the nucleus.

Supporting Information (see footnote on the first page of this article): Experimental procedures for the synthesis of the compounds, Tables S1 and S2 containing crystal data for **6**, **6′**, $\mathbf{L^{DQA}}$, [Re($\mathbf{L^{NPG}}$)(CO)$_3$]Cl, and [Re($\mathbf{L^{DPA}}$)(CO)$_3$]Cl, and Figures S1–S98.

Acknowledgments

This work was supported by the Nara Women's University Intramural Grant for Project Research, Grant-in Aid for Scientific Research from the Ministry of Education, Culture, Sports, Science and Technology (MEXT), Japan, and the Research for Promoting Technological Seeds and the A-STEP FS Stage, JST.

[1] a) K. J. Jensen, J. Brask, *Biopolymers (Peptide Sci.)* **2005**, *80*, 747–761; b) J. J. Reina, J. Rojo, *Tetrahedron Lett.* **2006**, *47*, 2475–2478; c) M. Diéguez, O. Pamies, C. Claver, *Chem. Rev.* **2004**, *104*, 3189–3216; d) S. Yano, Y. Mikata, *Bull. Chem. Soc. Jpn.* **2002**, *75*, 2097–2113; e) M. Diéguez, O. Pamies, A. Ruiz, Y. Diaz, S. Castillon, C. Claver, *Coord. Chem. Rev.* **2004**, *248*, 2165–2192; f) M. Diéguez, C. Claver, O. Pamies, *Eur. J. Org. Chem.* **2007**, 4621–4634.

[2] a) M. Gottschaldt, U. Schubert, *Chem. Eur. J.* **2009**, *15*, 1548–1557; b) V. Ladmiral, E. Melia, D. M. Haddleton, *Eur. Polym. J.* **2004**, *40*, 431–449; c) Y. Mikata, Y. Onchi, K. Tabata, S. Ogura, I. Okura, H. Ono, S. Yano, *Tetrahedron Lett.* **1998**, *39*, 4505–4508; d) Y. Mikata, Y. Shinohara, K. Yoneda, Y. Nakamura, K. Esaki, M. Tanahashi, I. Brudziñska, S. Hirohara, M. Yokoyama, K. Mogami, T. Tanase, T. Kitayama, K. Takashiba, K. Nabeshima, R. Takagi, M. Takatani, T. Okamoto, I. Kinoshita, M. Doe, A. Hamazawa, M. Morita, F. Nishida, T. Sakakibara, C. Orvig, S. Yano, *J. Org. Chem.* **2001**, *66*, 3783–3789; e) T. Storr, Y. Sugai, C. A. Barta, Y. Mikata, M. J. Adam, S. Yano, C. Orvig, *Inorg. Chem.* **2005**, *44*, 2698–2705.

[3] R. Alberto, R. Schibli, R. Waibel, U. Abram, A. P. Schubiger, *Coord. Chem. Rev.* **1999**, *190–192*, 901–919.

[4] a) M. L. Bowen, C. Orvig, *Chem. Commun.* **2008**, 5077–5091; b) M. Gottschaldt, D. Koth, D. Müller, I. Klette, S. Rau, H. Görls, B. Schäfer, R. P. Baum, S. Yano, *Chem. Eur. J.* **2007**, *13*, 10273–10280; c) M. Gottschaldt, C. Bohlender, D. Müller, I. Klette, R. P. Baum, S. Yano, U. S. Schubert, *Dalton Trans.* **2009**, 5148–5154; d) D. J. Yang, C.-G. Kim, N. R. Schechter, A. Azhdarinia, D.-F. Yu, C.-S. Oh, J. L. Bryant, J.-J. Won, E. E. Kim, D. A. Podoloff, *Radiology* **2003**, *226*, 465–473; e) T. Storr, M. Obata, C. L. Fisher, S. R. Bayly, D. E. Green, I. Brudziñska, Y. Mikata, B. O. Patrick, M. J. Adam, S. Yano, C. Orvig, *Chem. Eur. J.* **2005**, *11*, 195–203; f) T. Storr, C. L. Fisher, Y. Mikata, S. Yano, M. J. Adam, C. Orvig, *Dalton Trans.* **2005**, 654–655; g) C. L. Ferreira, F. L. N. Marques, M. R. Y. Okamoto, A. H. Otake, Y. Sugai, Y. Mikata, T. Storr, M. L. Bowen, S. Yano, M. J. Adam, R. Chammas, C. Orvig, *Appl. Radiat. Isot.* **2010**, *68*, 1087–1093; h) M. L. Bowen, N. C. Lim, C. B. Ewart, R. Misri, C. L. Ferreira, U. Häfeli, M. J. Adam, C. Orvig, *Dalton Trans.* **2009**, 9216–9227; i) C. L. Ferreira, C. B. Ewart, S. R. Bayly, B. O. Patrick, J. Steele, M. J. Adam, C. Orvig, *Inorg. Chem.* **2006**, *45*, 6979–6987; j) M. L. Bowen, Z.-F. Chen, A. M. Roos, R. Misri, U. Häfeli, M. J. Adam, C. Orvig, *Dalton Trans.* **2009**, 9228–9236; k) E. Benoist, Y. Coulais, M. Almant, J. Kovensky, V. Moreau, D. Lesur, M. Artigau, C. Picard, C. Galaup, S. G. Gouin, *Carbohydr. Res.* **2011**, *346*, 26–34.

[5] A. Salas-Burgos, P. Iserovich, F. Zuniga, J. C. Vera, J. Fischbarg, *Biophys. J.* **2004**, *87*, 2990–2999.

[6] R. Schibli, C. Dumas, J. Petrig, L. Spadola, L. Scapozza, E. Garcia-Garayoa, A. P. Schubiger, *Bioconjugate Chem.* **2005**, *16*, 105–112.

[7] Y. Du, R. J. Linhardt, *Tetrahedron* **1998**, *54*, 9913–9959.

[8] Y. Mikata, Y. Sugai, M. Obata, M. Harada, S. Yano, *Inorg. Chem.* **2006**, *45*, 1543–1551.

[9] S. Tzanopoulou, I. C. Pirmettis, G. Patsis, M. Paravatou-Petsotas, E. Livaniou, M. Papadopoulos, M. Pelecanou, *J. Med. Chem.* **2006**, *49*, 5408–5410.

[10] a) J. Petrig, R. Schibli, C. Dumas, R. Alberto, P. A. Schubiger, *Chem. Eur. J.* **2001**, *7*, 1868–1873; b) S. Orlandi, R. Annunziata, M. Benaglia, F. Cozzi, L. Manzoni, *Tetrahedron* **2005**, *61*, 10048–10060.

[11] Y. Mikata, S. Fujii, M. Naemura, K. Takahashi, Y. Noguchi, *Dalton Trans.* **2009**, 10305–10310.

[12] M. L. Sinnott, G. T. Tzotzos, S. E. Marshall, *J. Chem. Soc. Perkin Trans. 2* **1982**, 1665–1670.

[13] S. Pal, M. K. Chan, W. H. Armstrong, *J. Am. Chem. Soc.* **1992**, *114*, 6398–6406.

[14] K. A. Stephenson, S. R. Banerjee, T. Besanger, O. O. Sogbein, M. K. Levadala, N. McFarlane, J. A. Lemon, D. R. Boreham, K. P. Maresca, J. D. Brennan, J. W. Babich, J. Zubieta, J. F. Valliant, *J. Am. Chem. Soc.* **2004**, *126*, 8598–8599.

[15] a) Y. Mikata, M. Wakamatsu, A. Kawamura, N. Yamanaka, S. Yano, A. Odani, K. Morihiro, S. Tamotsu, *Inorg. Chem.* **2006**, *45*, 9262–9268; b) Y. Mikata, A. Yamashita, A. Kawamura, H. Konno, Y. Miyamoto, S. Tamotsu, *Dalton Trans.* **2009**, 3800–3806; c) Y. Mikata, A. Yamashita, K. Kawata, H. Konno, S. Itami, K. Yasuda, S. Tamotsu, *Dalton Trans.* **2011**, *40*, 4059–4066; d) Y. Mikata, A. Yamashita, K. Kawata, H. Konno, S. Itami, K. Yasuda, S. Tamotsu, *Dalton Trans.* **2011**, *40*, 4976–4981.

Received: September 8, 2011
Published Online: December 7, 2011

